

This work was written as part of one of the author's official duties as an Employee of the United States Government and is therefore a work of the United States Government. In accordance with 17 U.S.C. 105, no copyright protection is available for such works under U.S. Law.

Public Domain Mark 1.0

<https://creativecommons.org/publicdomain/mark/1.0/>

Access to this work was provided by the University of Maryland, Baltimore County (UMBC) ScholarWorks@UMBC digital repository on the Maryland Shared Open Access (MD-SOAR) platform.

Please provide feedback

Please support the ScholarWorks@UMBC repository by emailing scholarworks-group@umbc.edu and telling us what having access to this work means to you and why it's important to you. Thank you.

Effects of Lattice Strain and Band Offset on Electron Transfer Rates in Type-II Nanorod Heterostructures

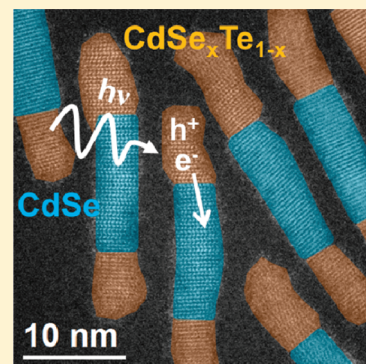
Hunter McDaniel,^{*,†,§} Matthew Pelton,[‡] Nuri Oh,[†] and Moonsub Shim^{*,†}

[†]Department of Materials Science and Engineering, University of Illinois, Urbana, Illinois 61801, United States

[‡]Center for Nanoscale Materials, Argonne National Laboratory, Argonne, Illinois 60439, United States

Supporting Information

ABSTRACT: Type-II nanorod heterostructures (NRHs) exhibit efficient directional charge separation and provide the potential to control this flow of charges through changes in structure and composition. We use transient-absorption spectroscopy to investigate how the magnitude of band offset and lattice strain alters dynamics of photogenerated electrons in CdSe/CdTe type-II NRHs. In the absence of alloying and strain effects, electron transfer occurs in ~ 300 fs. Reducing the conduction band offset by means of alloying leads to an even shorter charge-separation time (< 200 fs), whereas curved NRHs with pronounced strain exhibit a longer charge-separation time of ~ 700 fs.



SECTION: Physical Processes in Nanomaterials and Nanostructures

A critical aspect of any electronic device, be it a light-emitting diode, a field effect transistor, or a solar cell, is the control over the flow of charges. Many device architectures rely on semiconductor heterojunctions to direct charge carriers.¹ A type-I heterojunction confines both electrons and holes to the material with a smaller band gap, whereas a type-II or staggered band offset separates them. A type-III or broken gap offset can lead to tunnel junctions. Heterostructures of colloidal nanocrystals, especially those exhibiting anisotropic shapes such as nanorod heterostructures (NRHs),^{2–6} are beginning to allow these band engineering approaches to be applicable in versatile solution-processable materials. However, the band structure is greatly modified and complicated by quantum confinement, lattice strain, and large surface and interface area to volume ratios.^{7–9} These characteristics can provide tunability of properties of materials with nanometer dimensions, and exploiting them synergistically with the benefits of heterojunctions requires the understanding of how carrier separation is affected by them. Heterostructured nanocrystals of materials that form a type-II band offset, such as CdSe and CdTe,¹⁰ are of special interest in solar energy applications. The benefit of efficient carrier separation in type-II NRHs for photovoltaics has recently been demonstrated.¹¹ However, the dependence of this carrier separation on different morphologies, lattice strain, and composition has yet to be explored.

Transient changes in the optical absorption of nanocrystals upon photoexcitation can provide a wealth of information on photophysical processes, including exciton–exciton interactions and Auger recombination.^{12,13} Recently, transient-absorption (TA) measurements have been used to examine photoinduced

charge separation in type-II and quasi-type-II NRHs.^{14–20} Ultrafast electron-transfer rates have been measured, with charge-separation times of ~ 500 fs in CdSe/CdTe NRHs¹⁵ and < 350 fs in CdS/ZnSe NRHs.²⁰ Here we report the results of TA measurements on type-II CdSe/CdTe and related NRHs to show that both band offset and lattice strain have a strong influence on charge transfer dynamics.

Three types of NRHs are compared: (1) CdTe/CdSe/CdTe rod/rod/rod, (2) CdSe_{0.5}Te_{0.5}/CdSe/CdSe_{0.5}Te_{0.5} rod/rod/rod, and (3) CdSe/CdTe core/partial-shell curved structures. (TEM images of the samples are shown in the Supporting Information.) We will refer to these structures as (1) linear, (2) alloyed, and (3) curved NRHs, respectively. Schematics of the NRHs and their static absorption spectra are shown in Figure 1a–c. Absorption spectra of the seed CdSe nanorods from which these NRHs are grown are also shown for comparison. All three samples exhibit, to a different degree, three key transitions: (I) the CdSe band-edge transition, (II) the CdTe (or CdSe_{0.5}Te_{0.5}) band-edge transition, and (III) the charge transfer (CT) transition which results in electrons in CdSe and holes in CdTe (or CdSe_{0.5}Te_{0.5}).^{10,21,22} Ultrafast electron-transfer rates in linear NRHs have previously been measured.¹⁵ We therefore use these structures as a “control” sample to which the other two can be compared. For both linear and alloyed NRHs, the effects of lattice strain are expected to be negligible due to their extremely abrupt junctions, with little or

Received: March 7, 2012

Accepted: April 9, 2012

Published: April 12, 2012

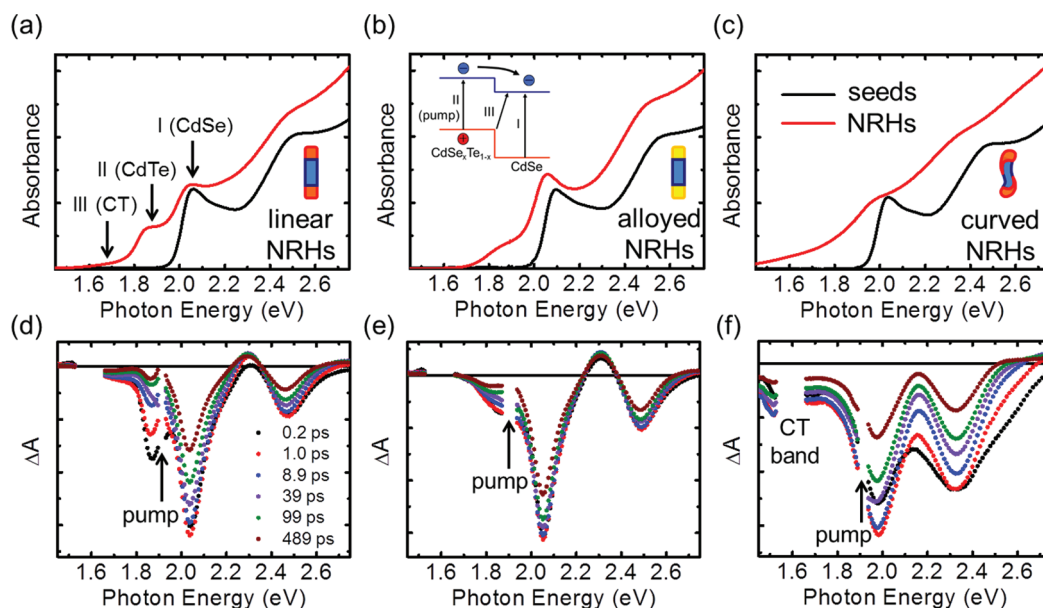


Figure 1. Linear absorption spectra of linear (a), alloyed (b), and curved (c) nanorod heterostructures (red) and the corresponding CdSe nanorod seeds (black). The three primary transitions of interest are labeled in (a) CdSe band edge (I), CdTe band edge (II), and CT band (III). The CdSe/CdSe_xTe_{1-x} band diagram is shown qualitatively in the inset to (b) with the primary transitions I, II, and III illustrated. Schematics of each of the NRHs are shown in the insets. Transient-absorption spectra for the same linear (d), alloyed (e), and curved (f) NRHs pumped with 1.91 eV photons for different pump–probe delays (indicated in legend in panel d).

no lattice distortion more than two atomic layers from the heterointerface.^{5,23} Relatively minor changes in the CdSe band-edge absorption feature upon CdTe or CdSe_{0.5}Te_{0.5} growth at the tips of the rods, as shown in Figure 1, provide further support that strain effects are negligible in these NRHs. Hence, comparison between linear and alloyed NRHs should reveal how the magnitude of the conduction-band offset alters the electron transfer rate, with minimal complications from other factors such as lattice strain and size effects. Comparison of the curved NRHs to the linear NRHs allows us to examine how the charge separation process is affected by a large and unusual lattice strain while holding the composition constant.

Figure 1d–f shows the TA spectra of NRHs. The pump photon energy is fixed at 1.91 eV, corresponding to excitation of the CdTe or CdSe_{0.5}Te_{0.5} tips. Low pump power is used to ensure that the measurements are well within the single-exciton regime. Little or no direct excitation of the larger-bandgap CdSe component should occur, with the possible exception of the curved NRHs: the curved structures have significantly broader absorption features, presumably due to strain gradients within the NRHs and increased structural inhomogeneity in the sample.²³ The primary features in the transient spectra are absorption bleaches (negative peaks reflecting reduced absorption) at the three transition energies discussed above. These bleach signals are primarily due to state-filling effects, that is, population of states by photogenerated carriers preventing additional absorption into those states. The peak near the pump photon energy (e.g., the peak at ~1.88 eV for linear NRHs and the shoulder near ~1.91 eV for alloyed NRHs) is the bleach of the CdTe (or CdSe_{0.5}Te_{0.5}) band edge transition. The most prominent peak, near 2.07 eV in linear NRHs, is attributed to the bleach of the CdSe band edge transition, which arises from electron transfer from the CdTe (or CdSe_{0.5}Te_{0.5}) conduction band to the lower energy CdSe conduction band across the interface.¹⁵ The strong bleach at photon energies higher than the pump contrasts non-

heterostructured (single-component) nanorods of CdSe and CdTe, where the largest bleach is observed around the band edge transition, below the pump energy. (See the Supporting Information.) The bleach at photon energies less than 1.77 eV is attributed to the CT band. This feature is most prominent in the curved NRHs, which exhibit the largest oscillator strength for this transition, as shown in Figure 1c. The larger oscillator strength for the CT transition in curved NRHs is most likely due to their larger interface area.^{5,11} The highest energy features (above ~2.20 eV) are attributed to higher CdSe transitions (i.e., “1P”). Unlike the lower-energy bleach signals, this feature, exhibiting both bleach and induced absorption, is characteristic of a peak shift due to the quantum-confined Stark effect. The large local electric field associated with separation of photo-excited charges in the type-II NRHs is expected to produce such a pronounced Stark shift.

With all of the main TA features identified, we now discuss electron transfer dynamics. On short (<3 ps) time scales, the bleach of the band-edge transition of single-component CdSe and CdTe nanorods is unchanged, apart from a fast rise within the instrument response time (see the Supporting Information). Charge trapping and recombination processes occur on a longer time scale of tens to hundreds of picoseconds. There has been a suggestion of charge separation across the type-II heterointerfaces reducing interactions of carriers with non-radiative/surface relaxation pathways, and indeed the observed bleach decay times have been reported to increase rather than decrease compared with those of single component nanorods.¹⁴ Thus, any spectral changes within the first ~2 ps of the pump (other than the initial fast/near-instantaneous buildup of the bleach and Stark shifts) observed in the NRHs can be attributed to charge transfer between CdSe and CdTe. Within these time scales, the lowest-energy CdSe transition and the CT transition in linear NRHs exhibit only a buildup of the bleach, consisting of an instrument-response limited rise followed by a somewhat slower component (<0.5 ps). The

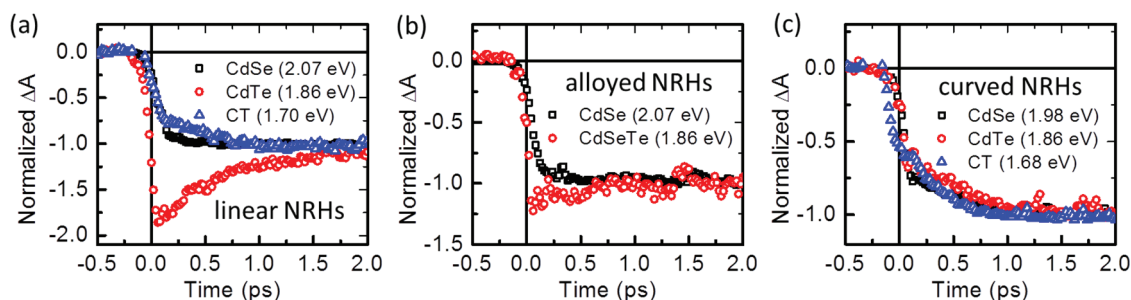


Figure 2. Short-delay transient bleach kinetics for linear (a), alloyed (b), and curved (c) nanorods heterostructures pumped at 1.91 eV by a ~ 200 fs pulse. The lowest-energy CdSe (black), CdTe (or $\text{CdSe}_{0.5}\text{Te}_{0.5}$) (red), and charge-transfer-band (blue) signals are probed at the indicated wavelengths. The time traces are normalized so that $\Delta A = -1$ at 2 ps. Time zero is set by the estimated peak of the pump signal and set to be the same for each measurement. The data have been corrected for chirp in the probe and have been binned in probe energy. Kinetics for the charge-transfer band of the alloyed NRHs is not shown due to weak signal, consistent with the expected quasi-type-II band offset.

CdTe band edge transition shows an initial fast buildup, but nearly 50% of the bleach recovers within 2 ps delay of the pump (Figure 2a). These results are consistent with the findings of ref 15, where the rise of the CdSe and CT bleach and the recovery of the CdTe bleach are attributed to electron transfer from CdTe to CdSe. The alloyed NRHs show qualitatively the same behavior, but the magnitudes are different and the rates appear to be faster.

The temporal response of the curved NRHs is qualitatively different: all spectral regions corresponding to CdSe band edge, CdTe band edge, and CT transitions show a similar, rising bleach. We suspect that one reason for this distinctly different response of curved NRHs is the broader absorption features; that is, the 1.91 eV pump can excite all three transitions. (See Figure 1.) Furthermore, the larger contribution of CT absorption in the curved NRHs (Figure 1c) means that the bleach signal of this feature is also more pronounced, so that the decaying signal at the CdTe transition energy can no longer be separately resolved. We nonetheless argue that the transient response within the first 2 ps after excitation is due to the electron-transfer process from CdTe to CdSe, similar to the other two NRHs studied. If the CT band were directly excited, then we would expect no significant subpicosecond dynamics in the TA signal other than the initial instrument-response-limited bleach buildup. If the CdSe band edge transition were directly excited, then there would be a hole transfer process that may also occur within the first 2 ps. However, the much higher density of states of the valence band means that the contribution of the hole to the transient bleach is much smaller than that of the electron.

To quantify charge transfer rates, we perform global analysis, fitting multiple-exponential functions over the entire temporal and spectral range measured.²⁴ In each case, we use the smallest number of principle components and the smallest number of time constants that give a good fit to the data. We begin by globally fitting the single-component (nonheterostructured) CdTe nanorod TA data (Figure 3a). Two time constants (10 and 103 ps) are obtained from this fit, representing carrier-trapping processes. In addition, there is a nearly constant term over the 500 ps measurement window, representing a much slower recombination process. The best fits of all NRH data, by contrast, require three time constants, in addition to the nearly constant term. We fix two of the time constants to be equal to those obtained for the CdTe nanorods, thereby obtaining one new time constant for each of the NRHs. These new time constants are 270 ± 110 fs for linear NRHs, 190 ± 150 fs for

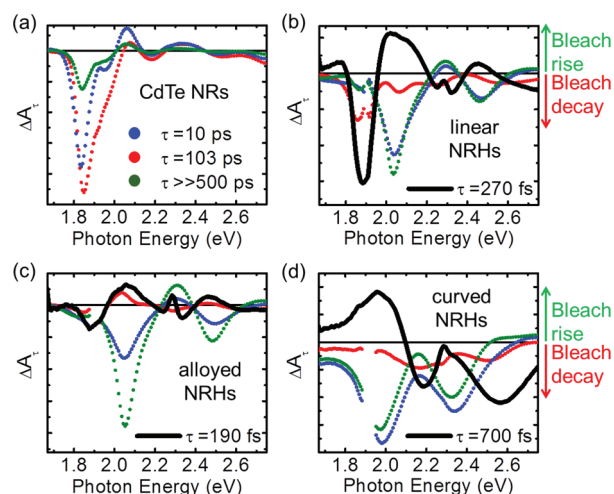


Figure 3. Coefficients obtained by global fitting of transient-absorption data for CdTe nanorods (a), linear NRHs (b), alloyed NRHs (c), and curved NRHs (d). Corresponding exponential time constants are indicated in the Figures. Negative values indicate a decaying bleach feature (or rising induced absorption), whereas positive values indicate a rising bleach feature (or decaying induced absorption). The pump photon energy was 1.91 eV in each case.

alloyed NRHs, and 700 ± 130 fs for curved NRHs. We note that allowing all three time constants to vary during the fits gives very similar results, indicating that trapping processes are nearly identical among all samples. Keeping the 10 and 103 ps time constants fixed reduces the number of free parameters in the fit and gives more stable results for the femtosecond scale time constants.

Figure 3 shows the coefficients for each exponential term as a function of the probe photon energy. The slower terms simply correspond to decaying bleach at each of the transition energies and thus reflect loss of carriers through either trapping or recombination. By contrast, the ultrafast term for the linear and alloyed NRHs shows a decay at the CdTe transition energy and a correlated rise at the CdSe and CT energies, as expected for electron transfer from CdTe to CdSe. In other words, the global analysis supports our previous interpretation of the transient kinetics. For the curved NRHs, the decay at the CdTe transition energy is no longer resolved, but the ultrafast component is still attributable to charge separation, as discussed above.

The faster electron transfer rate observed in alloyed NRHs may be understood intuitively by considering the wave function

overlap between electron states in the CdTe (or CdSe_{0.5}Te_{0.5}) and in CdSe. Lowering the conduction band edge of CdTe by alloying leads to greater penetration of the electron wave functions from one part of the heterostructure into another, thereby increasing the matrix element for transitions between the two states. Given the ultrafast electron transfer rate and the apparent overlap between the CdSe_{0.5}Te_{0.5} exciton peak and the CT band in the linear absorption spectrum, we suspect that the alloyed NRHs are approaching the quasi-type-II band offset regime; that is, the electron wave function is delocalized over nearly the entire NRH, whereas the hole state remains localized at the tips. This is consistent with the small magnitude of the quickly decaying feature at the CdTe band edge for the alloyed NRHs. (See Figures 2b and 3c.) Within the Marcus charge-transfer model proposed by Scholes et al.²⁵ our observations are consistent with electron transfer in the barrierless regime, where the mixing of the CdTe (or CdSe_{0.5}Te_{0.5}) exciton state with the CT state is invoked.

The effect of strain on the band energies in CdSe and CdTe is nontrivial,^{8,26–29} particularly in the presence of 3-D gradients in the strain. This makes it difficult to put forth a simple theoretical explanation of how lattice strain decreases the electron transfer rate in the curved NRHs. Intuitively, band bending due to compressive strain on CdTe is likely to produce an effective barrier at the CdSe/CdTe interface, reducing electron wave function overlap between the two regions and inhibiting charge transfer. However, the curved and linear NRHs also have different shapes; therefore, geometric effects, independent of strain, may also play a role in the charge-separation rate. With the partial side growth of CdTe, the heterointerface of curved NRHs should involve different crystal facets, which may also alter the effective band offset and the charge separation rate. Whereas further work is necessary to verify the mechanism, it is apparent that the effect in the strained NRHs is large, with the electron transfer time more than double that in the linear NRHs.

In summary, we have used TA spectroscopy to identify factors that significantly modify the ultrafast (~300 fs) electron transfer rates in CdSe/CdSe_xTe_{1–x} NRHs. Reducing the band offset by alloying leads to faster electron transfer (<200 fs), most likely due to the increasing wave function overlap between CdSe and CdSe_xTe_{1–x} conduction band states. Highly strained core/partial-shell curved NRHs exhibit significantly slower electron transfer (~700 fs), which is consistent with a barrier at the interface or at least reduced electron–hole wave function overlap caused by strain-induced band bending. These charge separation rates that can be varied by composition and lattice strain remain much faster than competing trapping and recombination processes. For photovoltaic applications, the negative effects of reduced electron transfer rate in curved NRHs may be more than offset by their enhanced CT absorption band.

METHODS

The single-pot synthesis was developed based on previous reports,⁵ and the details can be found in the Supporting Information. After cleaning by precipitation with methanol/butanol, all samples were dissolved in anhydrous toluene and immediately stored under N₂ in a desiccator. Measurements were conducted within 3 days of synthesis, and samples were stirred to reduce photocharging. Pump and probe pulses were generated from an amplified Ti/sapphire pulse, 10% of the power for a white light continuum (1.65 to 2.82 eV) for the

probe and 90% of the power for the pump. The pump power was kept at 250 μW, which corresponds to 150 nJ/pulse, to ensure <1 electron–hole pair per nanorod. When pump power was varied between 100 and 500 μW, TA spectra/kinetics remained unchanged. Global fitting analyses were carried out using Surface Explorer Pro software provided by Ultrafast Systems. Details of measurements and analysis are given in the Supporting Information.

ASSOCIATED CONTENT

Supporting Information

Experimental procedures, transient-absorption data for single-component CdSe and CdTe nanorods, and transmission electron microscope images. This material is available free of charge via the Internet at <http://pubs.acs.org>.

AUTHOR INFORMATION

Corresponding Author

*E-mail: hunter@lanl.gov; mshim@illinois.edu.

Present Address

[§]Center for Advanced Solar Photophysics, C-PCS, Chemistry Division, Los Alamos National Laboratory, Los Alamos, New Mexico 87545, United States.

Notes

The authors declare no competing financial interest.

ACKNOWLEDGMENTS

This material is based on work partially supported by the NSF (grant nos. 09-05175 and 11-53081) and the University of Illinois. Experiments were partially carried out in the Frederick Seitz Materials Research Laboratory Central Facilities, University of Illinois. Use of the Center for Nanoscale Materials was supported by the U.S. Department of Energy, Office of Science, Office of Basic Energy Sciences under contract no. DE-AC02-06CH11357.

REFERENCES

- (1) Kroemer, H. Nobel Lecture: Quasielectric Fields and Band Offsets: Teaching Electrons New Tricks. *Rev. Modern Phys.* **2001**, *73*, 783–793.
- (2) Shieh, F.; Saunders, A. E.; Korgel, B. A. General Shape Control of Colloidal CdS, CdSe, CdTe Quantum Rods and Quantum Rod Heterostructures. *J. Phys. Chem. B* **2005**, *109*, 8538–8542.
- (3) Halpert, J. E.; Porter, V. J.; Zimmer, J. P.; Bawendi, M. G. Synthesis of CdSe/CdTe Nanobarells. *J. Am. Chem. Soc.* **2006**, *128*, 12590–12591.
- (4) Carbone, L.; Nobile, C.; De Giorgi, M.; Della Sala, F.; Morello, G.; Pompa, P.; Hytch, M.; Snoeck, E.; Fiore, A.; Franchini, I. R.; et al. Synthesis and Micrometer-Scale Assembly of Colloidal CdSe/CdS Nanorods Prepared by a Seeded Growth Approach. *Nano Lett.* **2007**, *7*, 2942–2950.
- (5) McDaniel, H.; Zuo, J. M.; Shim, M. Anisotropic Strain-Induced Curvature in Type-II CdSe/CdTe Nanorod Heterostructures. *J. Am. Chem. Soc.* **2010**, *132*, 3286–3288.
- (6) Lo, S. S.; Mirkovic, T.; Chuang, C.-H.; Burda, C.; Scholes, G. D. Emergent Properties Resulting from Type-II Band Alignment in Semiconductor Nanoheterostructures. *Adv. Mater.* **2011**, *23*, 180–197.
- (7) Murray, C. B.; Norris, D. J.; Bawendi, M. G. Synthesis and Characterization of Nearly Monodisperse CdE (E = Sulfur, Selenium, Tellurium) Semiconductor Nanocrystallites. *J. Am. Chem. Soc.* **1993**, *115*, 8706–8715.
- (8) Smith, A. M.; Mohs, A. M.; Nie, S. Tuning the Optical and Electronic Properties of Colloidal Nanocrystals by Lattice Strain. *Nature Nanotechnol.* **2008**, *4*, 56–63.

- (9) Wang, S.; Wang, L.-W. Exciton Dissociation in CdSe/CdTe Heterostructure Nanorods. *J. Phys. Chem. Lett.* **2011**, *2*, 1–6.
- (10) Kim, S.; Fisher, B.; Eisler, H. J.; Bawendi, M. G. Type-II Quantum Dots: CdTe/CdSe(Core/Shell) and CdSe/ZnTe(Core/Shell) Heterostructures. *J. Am. Chem. Soc.* **2003**, *125*, 11466–11467.
- (11) McDaniel, H.; Heil, P. E.; Tsai, C.-L.; Kim, K.; Shim, M. Integration of Type II Nanorod Heterostructures into Photovoltaics. *ACS Nano* **2011**, *5*, 7677–7683.
- (12) Klimov, V. I. Spectral and Dynamical Properties of Multiexcitons in Semiconductor Nanocrystals. *Annu. Rev. Phys. Chem.* **2007**, *58*, 635–673.
- (13) Guyot-Sionnest, P.; Wehrenberg, B.; Yu, D. Intraband Relaxation in CdSe Nanocrystals and the Strong Influence of the Surface Ligands. *J. Chem. Phys.* **2005**, *123*, 074709.
- (14) Peng, P.; Milliron, D. J.; Hughes, S. M.; Johnson, J. C.; Alivisatos, A. P.; Saykally, R. J. Femtosecond Spectroscopy of Carrier Relaxation Dynamics in Type II CdSe/CdTe Tetrapod Heteronanostructures. *Nano Lett.* **2005**, *5*, 1809–1813.
- (15) Dooley, C. J.; Dimitrov, S. D.; Fiebig, T. Ultrafast Electron Transfer Dynamics in CdSe/CdTe Donor-Acceptor Nanorods. *J. Phys. Chem. C* **2008**, *112*, 12074–12076.
- (16) Lupo, M. G.; Sala, F. D.; Carbone, L.; Zavelani-Rossi, M.; Fiore, A.; Luer, L.; Polli, D.; Cingolani, R.; Manna, L.; Lanzani, G. Ultrafast Electron–Hole Dynamics in Core/Shell CdSe/CdS Dot/Rod Nanocrystals. *Nano Lett.* **2008**, *8*, 4582–4587.
- (17) Chuang, C.-H.; Lo, S. S.; Scholes, G. D.; Burda, C. Charge Separation and Recombination in CdTe/CdSe Core/Shell Nanocrystals as a Function of Shell Coverage: Probing the Onset of the Quasi Type-II Regime. *J. Phys. Chem. Lett.* **2011**, *1*, 2530–2535.
- (18) Zhu, H.; Song, N.; Lian, T. Wave Function Engineering for Ultrafast Charge Separation and Slow Charge Recombination in Type II Core/Shell Quantum Dots. *J. Am. Chem. Soc.* **2011**, *133*, 8762–8771.
- (19) She, C.; Demortiere, A.; Shevchenko, E. V.; Pelton, M. Using Shape to Control Photoluminescence from CdSe/CdS Core/Shell Nanorods. *J. Phys. Chem. Lett.* **2011**, *2*, 1469–1475.
- (20) Hewa-Kasakarage, N. N.; El-Khoury, P. Z.; Tarnovsky, A. N.; Kirsanova, M.; Nemitz, I.; Nemchinov, A.; Zamkov, M. Ultrafast Carrier Dynamics in Type II ZnSe/CdS/ZnSe Nanobarbells. *ACS Nano* **2010**, *4*, 1837–1844.
- (21) Milliron, D. J.; Hughes, S. M.; Cui, Y.; Manna, L.; Li, J. B.; Wang, L.-W.; Alivisatos, A. P. Colloidal Nanocrystal Heterostructures with Linear and Branched topology. *Nature* **2004**, *430*, 190–195.
- (22) Kumar, S.; Jones, M.; Lo, S. S.; Scholes, G. D. Nanorod Heterostructures Showing Photoinduced Charge Separation. *Small* **2007**, *3*, 1633–1639.
- (23) Shim, M.; McDaniel, H.; Oh, N. Prospects for Strained Type-II Nanorod Heterostructures. *J. Phys. Chem. Lett.* **2011**, *2*, 2722–2727.
- (24) Gampp, H.; Maeder, M.; Meyer, C. J.; Zuberbühler, A. D. Calculation of Equilibrium Constants from Multiwavelength Spectroscopic Data—I: Mathematical Considerations. *Talanta* **1985**, *32*, 95–101.
- (25) Scholes, G. D.; Jones, M.; Kumar, S. Energetics of Photoinduced Electron-Transfer Reactions Decided by Quantum Confinement. *J. Phys. Chem. C* **2007**, *111*, 13777–13785.
- (26) Yang, S.; Prendergast, D.; Neaton, J. B. Strain-Induced Band Gap Modification in Coherent Core/Shell Nanostructures. *Nano Lett.* **2010**, *10*, 3156–3162.
- (27) Sadowski, T.; Ramprasad, R. Core/Shell CdSe/CdTe Heterostructure Nanowires Under Axial Strain. *J. Phys. Chem. C* **2010**, *114*, 1773–1781.
- (28) Yadav, S. K.; Sadowski, T.; Ramprasad, R. Density Functional Theory Study of ZnX (X = O, S, Se, Te) under Uniaxial Strain. *Phys. Rev. B* **2010**, *81*, 144120.
- (29) Yang, S.; Prendergast, D.; Neaton, J. B. Nonlinear Variations in the Electronic Structure of II–VI and III–V Wurtzite Semiconductors with Biaxial Strain. *Appl. Phys. Lett.* **2011**, *98*, 152108.